with each other (Fig. 3, C and D). PGI and ALD are thought to be in vast excess relative to PFK (*21*), but some experimental data suggest that the relative in vivo activities of PGI and ALD are low enough for variations in these enzymes to be functionally relevant (*2*, *4*, *22*). These two enzymes flank PFK in the glycolytic pathway and thus their activities relative to that of PFK may affect flux. If PFK activities in *Fundulus* taxa are altered evolutionarily by allosteric modulation, then the correlation between PGI and ALD concentrations may reflect coordinate changes in PFK concentration or activity.

Which theory of metabolic flux best fits the observed evolutionary patterns? Adaptive variation in PYK concentration is expected under classical biochemical models because PYK catalyzes an irreversible adenosine 5′-triphosphate–producing reaction and experiences allosteric modulation. However, PFK, a regulatory enzyme, does not vary adaptively with temperature. Both LDH and GAPDH are equilibrium enzymes that are thought to be unable to affect flux. Our data indicate that these two equilibrium enzymes are adaptively important and thus affect metabolic flux. The coevolution of two pairs of equilibrium enzymes suggests that enzyme interactions (that is, epistasis between enzyme steps) may be as important as single enzymes for flux modulation. Thus, the data presented here suggest that many different enzymes modulate flux, supporting metabolic control theories.

REFERENCES AND NOTES

1. E. A. Newsholme and B. Crabtree, *J. Exp. Zool.* **239**, 159 (1986); B. Crabtree and E. A. Newsholme, *Biochem. J.* **247**, 113 (1987).
2. A. Cornish-Bowden and M. L. Cardenas, *Control of Metabolic Processes* (Plenum, New York, 1990).
3. H. Kacser and J. A. Burns, *Symp. Soc. Exp. Biol.* **27**, 65 (1973); M. A. Savageau and A. Sorribas, *J. Theor. Biol.* **141**, 93 (1989).
4. Y. Kashiwaya *et al.*, *J. Biol. Chem.* **269**, 25502 (1994).
5. A. L. Kruckeberg, H. E. Neuhaus, R. Feil, L. D. Gottlieb, M. Stitt, *Biochem. J.* **261**, 457 (1989).
6. The term "equilibrium enzymes" is used here to denote enzymes that catalyze reactions that proceed in either the forward or reverse direction depending on the relative concentrations of substrates and products. An alternative term is "intervening step enzyme."
7. G. Bernardi and D. A. Powers, *Copeia* **2**, 469 (1995).
8. R. C. Cashner, J. S. Rogers, J. M. Grady, in *Systematic, Historical Ecology and North American Freshwater Fishes*, R. L. Mayden, Ed. (Stanford Univ. Press, Stanford, CA, 1992), pp. 421–437.
9. E. O. Wiley, *Am. Zool.* **26**, 121 (1986).
10. P. W. Hochachka and G. N. Somero, *Biochemical Adaptation* (Princeton Univ. Press, Princeton, NJ, 1984).
11. G. N. Somero and S. C. Hand, *Physiol. Zool.* **63**, 443 (1990).
12. V. A. Pierce and D. L. Crawford, *Biochem. Genet.* **32**, 315 (1994); *Physiol. Zool.* **69**, 489 (1996).
13. Abbreviations for glycolytic enzymes: hexokinase (HK, E.C. 2.7.1.1), phosphoglucoisomerase (PGI, E.C. 5.3.1.9), phosphofructokinase (PFK, E.C. 2.7.1.11), aldolase (ALD, E.C. 4.1.2.13), triose-phosphate isomerase (TPI, E.C. 5.3.1.1), glyceraldehyde-3-phosphate dehydrogenase (GAPDH, E.C. 1.2.1.12), phosphoglycerokinase (PGK, E.C. 2.7.2.3), phosphoglyceromutase (PGM, E.C. 2.7.5.3), enolase (ENO, E.C. 4.2.1.11), pyruvate kinase (PYK, E.C. 2.7.1.40), lactate dehydrogenase (LDH, E.C. 1.1.1.27).
14. Phylogenetic autocorrelation is analogous to scaling on body mass and decomposes the measured variance in a trait into a phylogenetic and residual value for each taxon. Phylogenetic autocorrelation uses maximum likelihood methods to estimate ρ in the network model $y = \rho Wy + \varepsilon$, where y is the trait value for each taxon, W is the matrix containing information on phylogenetic relationships and distances, ρ is the autocorrelation coefficient, and ε is the taxon-specific residual for the trait. The true r^2 is calculated as 1 − (error variance/variance of Y) [J. M. Cheverud, M. M. Dow, W. Leutenegger, *Evolution* **39**, 1335 (1985); J. M. Cheverud and M. M. Dow, *Am. J. Phys. Anthropol.* **67**, 113 (1985); D. B. Miles and A. E. Dunham, *Am. Nat.* **139**, 848 (1992)].
15. Independent contrasts method assumes a Brownian motion model of evolution where variance in a trait increases through evolutionary time and calculates the amount of change between sister taxa at each node of the phylogeny. Independent contrasts are generated by subtracting trait values between all pairs of sister taxa in the tree. Contrasts are standardized by dividing by their standard deviation, calculated as the square root of the sum of branch lengths between the pair of taxa. Character displacement violates an assumption of this method, but in these data all ρ values are positive, suggesting no such violation [J. Felsenstein, *Am. Nat.* **125**, 1 (1985)].
16. T. Garland Jr., P. H. Harvey, A. R. Ives, *Syst. Biol.* **41**, 18 (1992).
17. T. Garland Jr. and C. M. Janis, *J. Zool.* **229**, 133 (1993).
18. D. Zahner and W. J. Malaisse, *Int. J. Biochem.* **25**, 1303 (1993).
19. D. K. Srivastava and S. A. Bernhard, *Annu. Rev. Biophys. Biophys. Chem.* **16**, 175 (1987).
20. F. Orosz, T. Y. Christova, J. Ovadi, *Biochem. Biophys. Res. Commun.* **147**, 1121 (1987).
21. B. Crabtree and E. A. Newsholme, *Biochem. J.* **126**, 49 (1972).
22. W. B. Watt, P. A. Carter, K. Donohue, *Science* **233**, 1187 (1986); W. B. Watt, *Am. Nat.* **125**, 118 (1985).
23. T. Garland Jr., A. W. Dickerman, C. M. Janis, J. A. Jones, *Syst. Biol.* **42**, 265 (1993).
24. National Oceanographic Data Center, *Water Temperature Guide to the Gulf Coast*, D. DeAngelis, Ed. (U.S. Department of Commerce, Washington, DC, 1982); *Water Temperature Guide to Atlantic Beaches*, D. DeAngelis, Ed. (U.S. Department of Commerce, Washington, DC, 1982).
25. Although the validity of either punctuational or gradual evolutionary models is unresolved, an assumption is required to statistically analyze these data. Both simulations and empirical studies suggest the phylogenetic methods used here are relatively insensitive to the assumption of punctuational models even when evolution is gradual [A. Purvis, J. L. Gittleman, H.-K. Luh, *J. Theor. Biol.* **167**, 293 (1994); M. Westneat, *Environ. Biol. Fishes* **44**, 263 (1995); J. L. Gittleman and H.-K. Luh, Eds., *Phylogenetics and Ecology; Joint Symposium Between the Natural History Museum and the Linnean Society of London* (Academic Press, London, 1994).
26. J. S. Rogers and R. C. Cashner, in *Community and Evolutionary Ecology of North American Stream Fishes*, W. J. Matthews and D. C. Heins, Eds. (Univ. of Oklahoma Press, Norman, OK, 1987), pp. 251–257; V. A. Lotrich, *Ecology* **56**, 191 (1975).
27. L. R. Parenti, *Bull. Am. Mus. Nat. Hist.* **168**, 335 (1981).
28. National Oceanic and Atmospheric Association, vol. 108, p. 15 (1994).

29. This project was aided by discussions with T. Garland, L. McIntyre, M. Westneat, E. Wiley, and J. Segal and by critical readings of the manuscript by A. Gibbs, S. Hand, R. Huey, and three anonymous reviewers. For help locating and obtaining species, we thank K. Able, L. Barnett, G. Byerly, R. Kneib, L. McKelvey, S. McMann, A. Pierce, M. Thayer, and E. Wiley; M. Eberle, and E. H. Edwards of the NC Parks Department; L. Fuiman and his lab; and the Department of Marine Resources at the Marine Biological Laboratory (Woods Hole, MA). Supported by NSF grant IBN-9419781 (to D.L.C.) and the Hinds Fund and Sigma Xi (to V.A.P.). V.A.P. is a Howard Hughes Medical Institute Predoctoral Fellow.

25 November 1996; accepted 20 February 1997

Synaptic Vesicle Endocytosis Impaired by Disruption of Dynamin–SH3 Domain Interactions

Oleg Shupliakov, Peter Löw, Detlev Grabs,* Helge Gad, Hong Chen, Carol David,† Kohji Takei, Pietro De Camilli,‡ Lennart Brodin‡

The proline-rich COOH-terminal region of dynamin binds various Src homology 3 (SH3) domain–containing proteins, but the physiological role of these interactions is unknown. In living nerve terminals, the function of the interaction with SH3 domains was examined. Amphiphysin contains an SH3 domain and is a major dynamin binding partner at the synapse. Microinjection of amphiphysin's SH3 domain or of a dynamin peptide containing the SH3 binding site inhibited synaptic vesicle endocytosis at the stage of invaginated clathrin-coated pits, which resulted in an activity-dependent distortion of the synaptic architecture and a depression of transmitter release. These findings demonstrate that SH3-mediated interactions are required for dynamin function and support an essential role of clathrin-mediated endocytosis in synaptic vesicle recycling.

The guanosine triphosphatase (GTPase) dynamin has an essential role in endocytosis (*1*, *2*). It forms a collar at the neck of endocytic pits and participates in the fission reaction that generates a free vesicle (*3*). Block of dynamin GTPase function in nerve terminals

leads to an arrest of endocytosis at the stage of invaginated endocytic pits and, as a consequence, to depletion of synaptic vesicles (*4*, *5*). Through distinct binding sites in its proline-rich COOH-terminal region, dynamin interacts with various SH3 domain–containing proteins (*6*). Here we present evidence of the importance of these interactions for dynamin function in living cells.

In nerve terminals, a major SH3 domain binding partner is amphiphysin (*7*, *8*), which binds dynamin at a single site comprising the sequence PSRPNR (*9*) near its COOH-terminus (*10*). Amphiphysin also binds the plasmalemmal clathrin adaptor AP-2 (*11*) through a site distinct from its SH3 domain (*8*). Therefore, amphiphysin may participate in recruiting dynamin to coated pits (*8*). To disrupt the interactions mediated by the amphiphysin binding site on dynamin, a fluorophore-conjugated glutathione-S-transferase (GST) fusion protein containing the SH3 domain of human amphiphysin (GST-amphSH3) (*12*) was injected presynaptically into the lamprey giant reticulospinal synapse (*13*–*15*). Injection did not alter the morphology of synapses maintained at rest (Fig. 1A) (*16*). The organization of synaptic vesicle clusters and the plasmalemma resembled that in normal synapses (*14*, *17*), and only a small number of coated pits were present (Fig. 2). However, when low-frequency action-potential stimulation (at 0.2 Hz for 30 min) was applied to stimulate synaptic vesicle exocytosis, the structure of the synapses changed dramatically (Fig. 1B). Many coated pits appeared (Figs. 1B and 2), which virtually covered the plasmalemma around the active zones within a radius of about 3 to 4 μm. Large plasmalemmal invaginations bearing coated pits were often visible at the margin of the synaptic regions (Fig. 1C), and the number of synaptic vesicles decreased (*18*). The remaning vesicles appeared to be organized normally in clusters anchored to the active zones (*19*). After more intense stimulation (at 5 Hz for 30 min) the synaptic ultrastructure was even more distorted (Fig. 1D). In addition to the abundant coated pits (Fig. 2), large numbers of tubular and sheetlike membrane invaginations extended into the axon and occupied a large part of the synaptic region. The number of synaptic vesicles was further reduced (*20*) and the presynaptic plasma membrane had expanded, as indicated by the formation of protrusions of the presynaptic compartment around the postsynaptic dendrites (Fig. 1D) (*21*). Moreover, the active zone area was now fragmented and appeared as irregular patches (Fig. 1D) interrupted by membrane invaginations bearing coated pits. The number of synaptic vesicles tethered to the active zone membrane was reduced (*22*).

Binding assays were done to verify that lamprey dynamin binds the SH3 domain of human amphiphysin in vitro (*23*). When a lamprey central nervous system (CNS) extract was affinity-purified onto GST-amphSH3 bound to glutathione-Sepharose, the predominant protein specifically bound to the beads comigrated with rat dynamin at about 100 kD (Fig. 3A) (*8*) and reacted with antibodies to dynamin (Fig. 3A). The binding to GST-amphSH3 was inhibited by a 15-oligomer peptide from human dynamin containing the amphSH3 binding site (Fig. 3B) (*10*, *24*). Binding was not detectable when a mutant amphiphysin SH3 domain (GST-amphSH3mut) was used (Fig. 3B). This protein has two point mutations at conserved amino acids in the SH3 domain ($Gly^{684} \rightarrow Arg^{684}$ and $Pro^{687} \rightarrow Leu^{687}$) that drastically reduce dynamin binding (*10*). In an overlay assay, GST-amphSH3 reacted primarily with a 100-kD band comigrating with dynamin, which was not recognized by

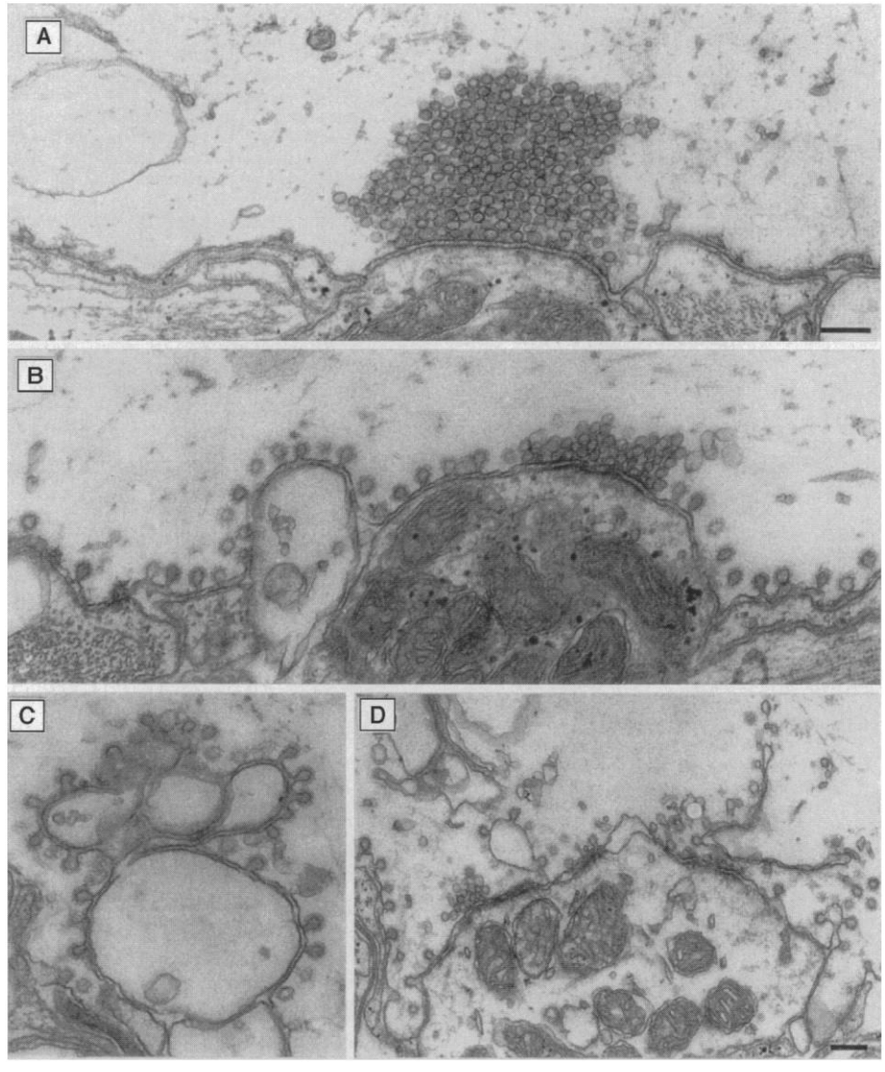

Fig. 1. Inhibition of synaptic vesicle recycling by GST-amphSH3. (**A**) A synapse in an axon maintained in low calcium solution (0.1 mM Ca^{2+} and 4 mM Mg^{2+}) without stimulation after injection of GST-amphSH3. (**B**) A synapse in an axon that was stimulated (in a solution containing 2.6 mM Ca^{2+} and 1.8 mM Mg^{2+}) at 0.2 Hz for 30 min after the injection of GST-amphSH3. (**C**) Membrane invaginations at the margin of a synaptic area in an axon treated as in (B). (**D**) A synapse in an axon stimulated at 5 Hz for 30 min after GST-amphSH3 injection. The number of coated pits for each condition is given in Fig. 2. Scale bars, 0.2 μm [bar in (A) applies to (A) through (C)].

O. Shupliakov, P. Löw, H. Gad, L. Brodin, The Nobel Institute for Neurophysiology, Department of Neuroscience, Karolinska Institutet, S-171 77 Stockholm, Sweden.
D. Grabs, H. Chen, C. David, K. Takei, P. De Camilli, Department of Cell Biology and Howard Hughes Medical Institute, Yale University School of Medicine, New Haven, CT 06510, USA.
*Present address: Institut für Anatomie/Charité, Philippstrasse 12, D-10115 Berlin, Germany.
†Present address: Department of Immunology, Weizmann Institute of Science, 76100 Rehovot, Israel.
‡To whom correspondence should be addressed. E-mail: pietro_decamilli@quickmail.yale.edu (for P. De Camilli); lennart.brodin@neuro.ki.se (for L. Brodin)

GST-amphSH3mut or by GST linked to SAP-90/PSD95, an SH3-containing protein that does not bind rat dynamin (*25*). Conversely, when lamprey CNS extract was affinity-purified on a GST fusion protein comprising the entire proline-rich domain of human dynamin (*26*), a band was affinity-purified that comigrated with rat brain amphiphysin and was recognized by monoclonal and polyclonal antibodies to amphiphysin (Fig. 3C) (*26*). This band was not present in material affinity-purified on a fusion protein containing a truncated proline-rich domain (Fig. 3C) devoid of the amphiphysin binding site (*10*).

To rule out the possibility that GST-amphSH3 simply impaired dynamin function rather than competed with an endogenous SH3 binding site in the living synapses, we microinjected the dynamin peptide used above (*27*). The peptide produced morphological alterations (Fig. 4, A and B) qualitatively similar to those observed after injection of GST-amphSH3. The synaptic regions showed an increase in the number of coated pits, and the plasma membrane exhibited invaginations bearing coated pits. Presynaptic injection of GST-amphSH3- mut had little effect on the synaptic ultrastructure (Fig. 4C; stimulation at 5 Hz). The number of coated pits was significantly lower than that in GST-amphSH3–injected axons and only slightly exceeded that in control axons (Fig. 2). The structure of the plasmalemma, synaptic vesicle clusters, and active zone region appeared normal (Fig. 4C). Injection of GST-SAP-90/PSD95 (Fig. 4D; stimulation at 5 Hz) or of GST alone (*28*) failed to induce obvious changes in the synaptic morphology with regard to synaptic vesicle clusters, the plasmalemma, and coated structures.

Analysis of serially sectioned synapses showed that coated membrane structures induced after injection of GST-amphSH3 or the dynamin peptide were always connected with the plasma membrane, whereas free coat-

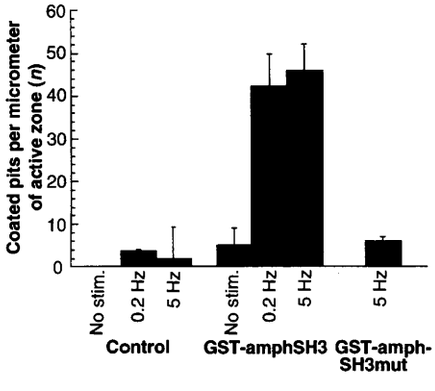

Fig. 2. Number of coated pits in synaptic areas of control axons and GST-amphSH3– and GST-amphSH3mut–injected axons. The values represent the number of coated pits in the center section of synapses ± SD. Control synapses were from uninjected axons adjacent to axons injected with GST-amphSH3. Synapses that were not stimulated (No stim.) were from axons maintained in 0.1 mM Ca and 4 mM Mg. In the control synapses that were not stimulated, no coated pits were observed. The effect of GST-amphSH3mut was only examined after stimulation at 5 Hz. The data for GST-amphSH3 and GST-amphSH3mut were obtained from axons in which the concentrations of the injected proteins in the axonal cytoplasm were similar, as judged from the fluorescence intensity after compensation for the dye-to-protein ratio; $n = 5$ synapses for each condition. The number of coated pits differed significantly between GST-amphSH3 with no stimulation and GST-amphSH3 at 0.2 Hz ($P < 0.005$) and 5 Hz ($P < 0.001$); between GST-amphSH3 at 5 Hz and GST-amphSH3mut at 5 Hz ($P < 0.001$); and between control at 5 Hz and GST-amphSH3mut at 5 Hz ($P < 0.05$). We assume that the lack of increase in coated pits between GST-amphSH3 at 0.2 Hz and at 5 Hz may reflect a saturation of the endocytic machinery.

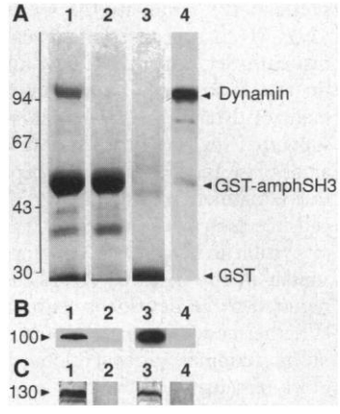

Fig. 3. Specificity of interaction between the proline-rich domain of dynamin and the SH3 domain of amphiphysin. (**A**) Binding of a 100-kD protein from lamprey spinal cord to GST-amphSH3. Eluates of proteins bound to GST-amphSH3 with lamprey extract added (lane 1), GST-amphSH3 with no extract added (lane 2), and GST alone with lamprey extract added (lane 3) (lanes 1 through 3 show Coomassie-stained gels). Lane 4 shows a protein immunoblot with dynamin antiserum DG1 (*10*) on material corresponding to lane 1 (*23*). (**B**) Blots with dynamin antiserum DG1 on lamprey proteins bound to GST-amphSH3 (lane 1), GST-amphSH3mut (lane 2) (lanes 1 and 2 run in parallel), GST-amphSH3 (lane 3), and GST-amphSH3 in the presence of 300 μM of dynamin peptide (lane 4) (lanes 3 and 4 run in parallel) (*24*). (**C**) Blots with monoclonal antibodies to the COOH-terminal portion of amphiphysin on proteins from rat brain (lanes 1 and 2) and from lamprey spinal cord (lanes 3 and 4) bound to GST fusion proteins containing the full-length dynamin proline-rich domain (lanes 1 and 3) or a truncated proline-rich domain lacking the binding site for amphiphysin (lanes 2 and 4) (*26*).

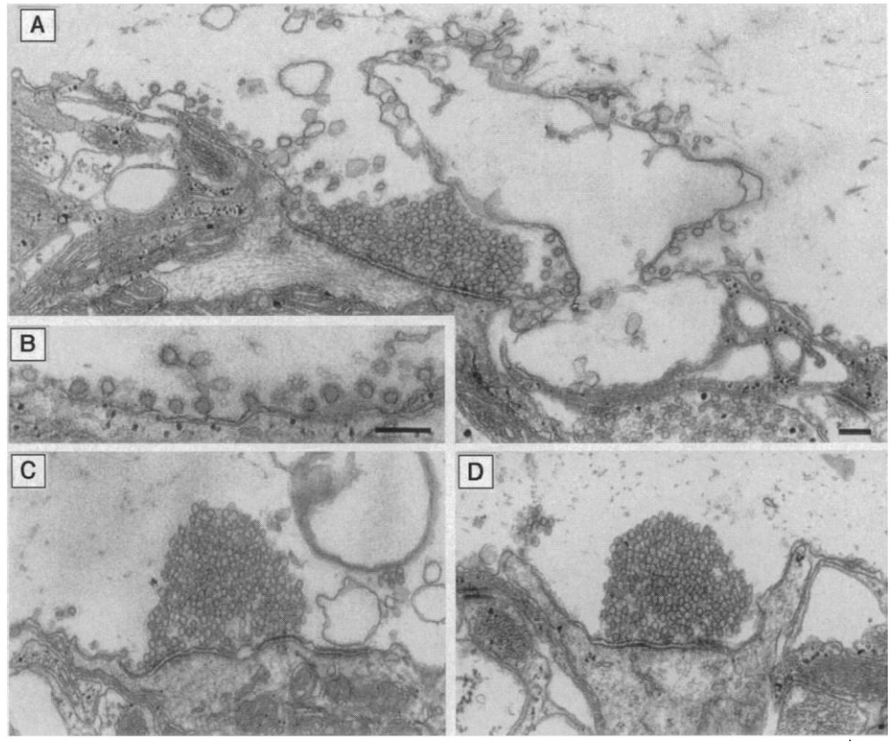

Fig. 4. Effects of a dynamin peptide and various fusion proteins on synaptic vesicle recycling. (**A** and **B**) Synaptic areas in axons injected with a 15-oligomer dynamin peptide (*24*). (**C** and **D**) Synapses injected with GST-amphSH3mut (C) and GST-SAP90/PSD95 (D). In (A) through (D), the axons were stimulated at 5 Hz for 30 min after the injection. Endosomes similar to those present in (C) were also observed in uninjected axons. Scale bars, 0.2 μm [bar in (A) applies to (A), (C), and (D)].

ed vesicles were not observed. Most coated pits had a small homogenous size and a narrow neck, which suggests arrest, or strong kinetic delay, of endocytosis at a late stage preceding fission. The extensive depletion of synaptic vesicles and the accumulation of invaginated endocytic pits observed in injected terminals was reminiscent of the morphological changes observed in the temperature-sensitive *Drosophila* mutant *shibire*, in which the mutation has been localized to the dynamin gene (*4*, *5*). However, the electron-dense dynamin collar that surrounds the neck of endocytic pits in *shibire* nerve terminals (*4*) was not present (*29*), which suggests that disruption of the dynamin-SH3 interaction may inhibit synaptic vesicle fission by preventing the recruitment of dynamin (*8*, *10*). This possibility is supported by our observation that GST-amphSH3 and the dynamin peptide inhibit the recruitment of dynamin to coated pits in a cell-free assay (*30*). Moreover, the endocytic pits visible in *shibire* nerve terminals, although similar in size to those described here, were reported to be devoid of clathrin coats (*4*). Whether endocytic pits become uncoated in *shibire* terminals after prolonged endocytic block remains unclear.

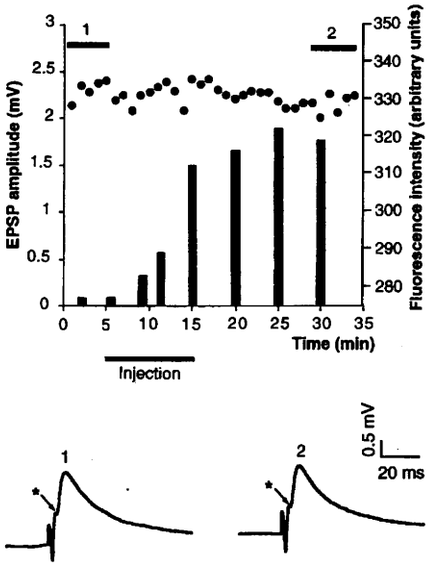

Fig. 5. Lack of effect of GST-amphSH3 on neurotransmitter release during low-frequency stimulation. An EPSP was evoked in a spinal neuron by 0.2 Hz stimulation of a giant reticulospinal axon by a microelectrode filled with Cy5-conjugated GST-amphSH3. The protein was injected with pressure pulses (injection). (**Top**) Bars represent the fluorescence intensity (in arbitrary units) in the area of the presynaptic axon where the release sites mediating the EPSP were located (*13*). The points represent 1-min averages of the total EPSP amplitude. (**Bottom**) The traces (1 and 2) are 5-min averages during the periods indicated. The electrotonic component of the mixed electrotonic-chemical EPSP (*13*) is indicated with an asterisk.

To test whether GST-amphSH3 alters neurotransmitter release we recorded intracellularly from spinal target cells while stimulating single reticulospinal axons (*13*, *17*). When excitatory postsynaptic potentials (EPSPs) were evoked by low-frequency stimulation (Fig. 5; 0.2 Hz), presynaptic injection of GST-amphSH3 did not alter the EPSP amplitude during an observation period of 30 min (*31*). This correlated with the lack of change in the number of synaptic vesicles tethered to active zones (*19*) and was consistent with the previously reported lack of correlation between the total vesicle pool and the EPSP amplitude (*17*). Thus GST-amphSH3 appears to interfere selectively with endocytosis, whereas it has no apparent direct effect on synaptic exocytosis (*32*). Under conditions of intense exocytosis, however, there was a marked reduction of the EPSP (Fig. 6A) (*33*) that by far exceeded the reduction observed normally at this level of sustained release (*34*). This correlated with the disruption of the active zone region (Fig. 6B) and the reduction in the number of synaptic vesicles tethered to the active zone membrane observed under these conditions (*22*). Thus the impairment of exocytosis appears to be a consequence of the changes in synaptic structure induced by GST-amphSH3 at high rates of release. EPSPs evoked from axons injected with GST-amphSH3mut (Fig. 6, A and C) or GST (Fig. 6A) were moderately reduced during stimulation at 5 Hz (*33*), similarly to those evoked from uninjected axons (*34*).

The ultrastructural and electrophysiological effects correlated with the targeting of fluorophore-conjugated injected proteins in the living axons as assessed by fluorescence microscopy. GST-amphSH3 accumulated in spots (Fig. 6D) with a location corresponding to that of synaptic release sites (*14*, *17*) where dynamin is accumulated (*35*). In contrast, GST-amphSH3mut remained diffuse within the axon (Fig. 6E), as did GST-SAP90 and GST alone (*36*).

Our results indicate that interaction of dynamin's proline-rich domain with an SH3 domain has a key role in the final steps of clathrin-coated vesicle formation. The

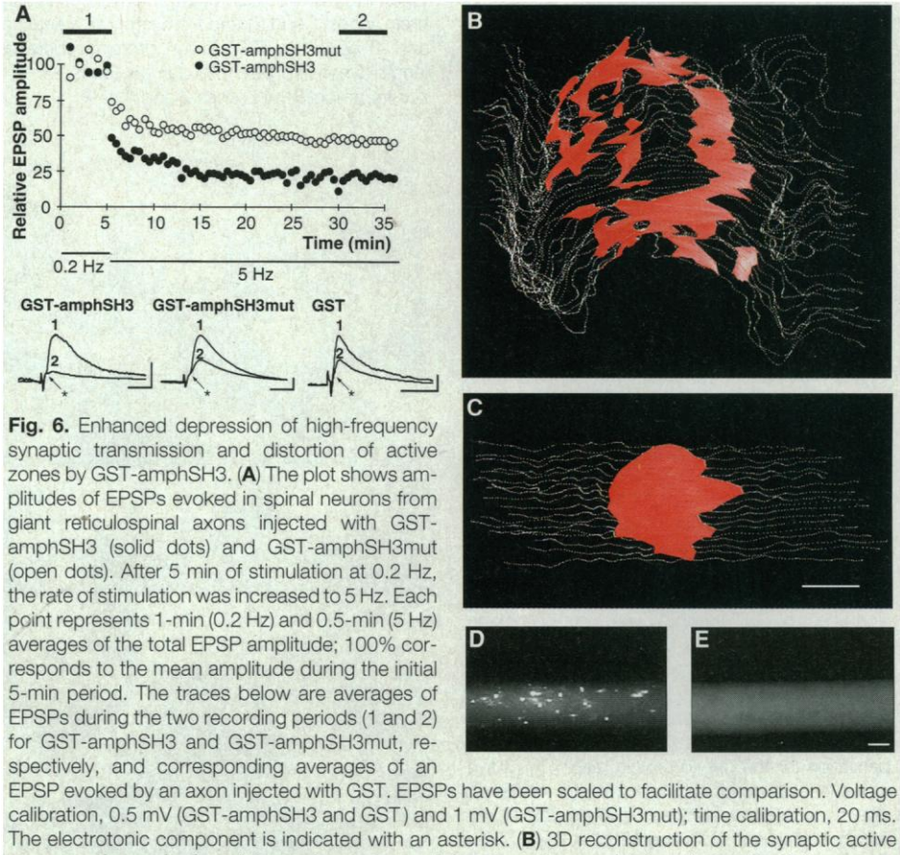

Fig. 6. Enhanced depression of high-frequency synaptic transmission and distortion of active zones by GST-amphSH3. (**A**) The plot shows amplitudes of EPSPs evoked in spinal neurons from giant reticulospinal axons injected with GST-amphSH3 (solid dots) and GST-amphSH3mut (open dots). After 5 min of stimulation at 0.2 Hz, the rate of stimulation was increased to 5 Hz. Each point represents 1-min (0.2 Hz) and 0.5-min (5 Hz) averages of the total EPSP amplitude; 100% corresponds to the mean amplitude during the initial 5-min period. The traces below are averages of EPSPs during the two recording periods (1 and 2) for GST-amphSH3 and GST-amphSH3mut, respectively, and corresponding averages of an EPSP evoked by an axon injected with GST. EPSPs have been scaled to facilitate comparison. Voltage calibration, 0.5 mV (GST-amphSH3 and GST) and 1 mV (GST-amphSH3mut); time calibration, 20 ms. The electrotonic component is indicated with an asterisk. (**B**) 3D reconstruction of the synaptic active zone membrane (red) and the main contours of the plasmalemma (white stippled lines) in an axon subjected to 30 min of stimulation at 5 Hz after injection of GST-amphSH3 (*42*). A transverse section of this synapse is illustrated in Fig. 1D. (**C**) 3D reconstruction of a synaptic active zone after injection of GST-amphSH3mut [stimulation was as in (B)]. (**D**) Image of a living reticulospinal axon, showing accumulation of fluorescence in spots corresponding to release sites (*17*) after injection of Cy5-linked GST-amphSH3 (*35*). (**E**) Image of fluorescence corresponding to Cy5-linked GST-amphSH3mut. Scale bar in (C), 0.5 μm; in (E), 10 μm.

critical region of dynamin involved in this interaction comprises the binding site for amphiphysin (*10*). Thus amphiphysin may act as a link between early and late stages in clathrin-coated vesicle formation, which enables the assembly of dynamin rings around their necks (*3*, *29*, *30*).

The role of coated vesicles in synaptic vesicle recycling has been a matter of debate (*37*). As shown here, after inhibition of the fission reaction, the role of the clathrin-coated vesicle pathway became evident during both low and high frequencies of stimulation. Thus the apparent lack of correlation between exocytosis and coated structures may be attributed to the short lifetime of the coated intermediates under normal conditions (*38*).

Although interaction with amphiphysin may have a major role in synaptic vesicle endocytosis, the interactions with other SH3 domain–containing proteins may act in concert with or substitute for this site in other endocytic reactions (*1*, *6*, *39*). For example, co-localization of dynamin and clathrin in COS cell membranes depends on a region of the proline-rich domain located upstream of the amphiphysin binding site (*40*).

REFERENCES AND NOTES

1. P. De Camilli and K. Takei, *Neuron* **16**, 481 (1996).
2. M. Robinson, *Curr. Opin. Cell. Biol.* **6**, 538 (1994).
3. K. Takei, P. S. McPherson, S. L. Schmid, P. De Camilli, *Nature* **374**, 186 (1995).
4. J. H. Koenig and K. Ikeda, *J. Neurosci.* **9**, 3844 (1989).
5. M. S. Chen *et al.*, *Nature* **351**, 583 (1991); A. M. Van Der Bliek and E. M. Meyerowitz, *ibid.*, p. 411.
6. I. Gout *et al.*, *Cell* **75**, 25 (1993); J. S. Herskovits, H. S. Shpetner, C. C. Burgess, R. B. Vallee, *Proc. Natl. Acad. Sci. U.S.A.* **90**, 11468 (1993); K. Seedorf *et al.*, *J. Biol. Chem.* **269**, 16009 (1994).
7. B. Lichte, R. W. Veh, H. E. Meyer, M. W. Kilimann, *EMBO J.* **11**, 2521 (1992).
8. C. David, P. McPherson, O. Mundigl, P. De Camilli, *Proc. Natl. Acad. Sci. U.S.A.* **93**, 331 (1996).
9. Single-letter abbreviations for the amino acid residues are as follows: A, Ala; G, Gly; N, Asn; P, Pro; Q, Gln; R, Arg; S, Ser; V, Val.
10. D. Grabs *et al.*, *J. Biol. Chem.*, in press.
11. L. H. Wang, T. C. Südhof, R. G. W. Andersson, *ibid.* **270**, 10079 (1995).
12. C. David, M. Solimena, P. De Camilli, *FEBS Lett.* **351**, 73 (1994).
13. L. Brodin, O. Shupliakov, J. Hellgren, V. A. Pieribone, R. H. Hill, *J. Neurophysiol.* **72**, 592 (1994).
14. O. Shupliakov, L. Brodin, S. Cullheim, O. P. Ottersen, J. Storm-Mathisen, *J. Neurosci.* **7**, 1111 (1992).
15. The giant reticulospinal axons in the lamprey spinal cord are unbranched and form glutamatergic synapses [AMPA (α-amino-3-hydroxy-5-methyl-4-isoxazole-propianate) and NMDA (*N*-methyl-D-aspartate) receptors] from their main trunk (diameter 30 to 50 μm) onto dendrites of spinal neurons (*13*, *14*). GST fusion proteins were prepared as described (*8*, *10*, *12*) and labeled with a monofunctional Cy5 dye (Amersham) according to the manufacturer's instructions. The dye-to-protein molar ratio was between 1.5 and 4. The labeled proteins [0.5 to 1.5 mg/ml in 250 mM K acetate and 10 mM Hepes (pH 7.4)] were injected with pressure pulses (5 to 15 psi) of 200 ms duration through micropipettes (with a resistance of 50 to 70 megohm) into giant reticulospinal axons (*13*) with a resting membrane potential of at least −60 mV. The protein-linked fluorescence was monitored with a charge-coupled device (CCD) detector cooled to −60°C (Princeton Instruments). The injection microelectrode was removed before stimulation was applied through an extracellular electrode (*13*). The stimulation period was ended by replacing the physiological solution (*21*) with fixative containing 3% glutaraldehyde and 0.5% *p*-formaldehyde in 0.1 M phosphate buffer (pH 7.4).
16. The preparations were processed as described (*21*). Synapses were cut in serial ultrathin sections and examined with a Philips CM12 electronmicroscope.
17. V. A. Pieribone *et al.*, *Nature* **375**, 493 (1995).
18. The total number of synaptic vesicles in synapses of GST-amphSH3–injected axons was 254 ± 75 (unstimulated) and 148 ± 67 (0.2 Hz stimulation) ($n = 4$ and 6, respectively; $P < 0.05$, t test). Values represent the average number of vesicles per micrometer of active zone in the center section of synapses ± SD. This value shows a linear correlation with the total number of synaptic vesicles per synapse (*21*).
19. The active zones exhibited a disk like shape, as described for normal synapses (*41*). The number of synaptic vesicles within 0 to 50 nm from the active zone membrane (the first row of vesicles) was 14 ± 3 and 13 ± 4 for GST-amphSH3 and control synapses, respectively. The number of vesicles in the 0- to 150-nm region was 43 ± 4 and 51 ± 4 for GST-amphSH3 and control synapses, respectively ($P < 0.05$, comparison of the latter two values; $n = 5$; t test).
20. The total number of synaptic vesicles per micrometer of active zone for GST-amphSH3–injected axons stimulated at 5 Hz was 58 ± 32 ($n = 6$), $P < 0.05$ (t test) in comparison with GST-amphSH3–injected axons stimulated at 0.2 Hz (*18*); $P < 0.001$ in comparison with GST-amphSH3–injected, unstimulated axons (*18*).
21. O. Shupliakov, V. A. Pieribone, H. Gad, L. Brodin, *Eur. J. Neurosci.* **7**, 1111 (1995).
22. The number of synaptic vesicles within 0 to 50 nm from the active zone membrane was 7 ± 3 and 14 ± 1, for GST-amphSH3–injected and control synapses, respectively (5 Hz stimulation; $P < 0.001$, $n = 5$, t test). The corresponding values for the 0- to 150-nm region were 20 ± 11 and 47 ± 5 ($P < 0.001$, $n = 6$; values represent synaptic vesicles per micrometer of active zone).
23. Lamprey spinal cords were homogenized (20% w/v) in a buffer containing 150 mM NaCl; 10 mM Hepes (pH 7.4); 5 mM EDTA; 4 μg/ml each of leupeptin, pepstatin, antipain and aprotinin; 10 mM benzamidine; and 0.4 mM phenylmethylsulfonyl fluoride. Triton X-100 (20% w/v) was added to the homogenate (for a final concentration of 1% w/v), which was agitated for 1 hour on ice. Insoluble material was removed at 40,000*g* for 1 hour at 4°C. The extract was incubated with glutathione-Sepharose beads and then with Sepharose beads (50 to 200 μl) bound with GST fusion protein for 2 hours at 4°C. The beads were then washed extensively with the buffer containing 1% w/v Triton X-100. The proteins were eluted with SDS–polyacrylamide gel electrophoresis sample buffer, and protein separation and immunoblotting was done as described (*8*, *10*).
24. The peptide PPPQVPSRPNRAPPG (*9*) corresponds to amino acids 828 to 842 of dynamin Iaa [J. M. Sontag *et al.*, *J. Biol. Chem.* **269**, 4547 (1994)]. In peptide competition assays, a final concentration of 300 μM was used. The peptide produced a similar inhibition of dynamin binding to GST-amphSH3 when rat brain extract was used (P. Löw, L. Brodin, D. Grabs, P. De Camilli, unpublished observation).
25. P. S. McPherson *et al.*, *Nature* **379**, 353 (1996).
26. Lamprey spinal cord extract was affinity-purified (*23*) with GST fusion proteins containing either the full-length proline-rich domain of dynamin Iaa or the proline-rich domain lacking the last 31 amino acids in the COOH-terminus (*10*). Monoclonal antibodies to the COOH-terminal portion of human amphiphysin (*12*) were from A. Zhang and M. Butler. Similar results were obtained with polyclonal antibodies to amphiphysin (M. Butler and P. De Camilli, unpublished observations).
27. The peptide (*24*) was mixed with injection solution (*15*) at a concentration of 20 mM with 5 μM Texas Red–conjugated dextran 3000 (Molecular Probes) added as an injection marker.
28. O. Shupliakov and L. Brodin, unpublished observation. See also (*17*) for other examples of control-injected synapses.
29. The electron-dense dynamin collars present in the *shibire* mutant are visible in specimens fixed and stained with the same methods used in the present study (*4*, *21*).
30. Recruitment of rat brain dynamin to endocytic sites in mammalian cell membranes under in vitro conditions is blocked by GST-amphSH3 and the 15-oligomer dynamin peptide (*24*), whereas the recruitment of the clathrin coat, as shown by AP180, amphiphysin, or clathrin labeling, is not affected (H. Chen, K. Takei, P. De Camilli, unpublished observations).
31. The total EPSP amplitude measured 26 to 30 min after GST-amphSH3 had reached the synaptic region in the presynaptic axon remained within ±22% of the amplitude during a 3- to 5- min control period before the injection (mean difference + 4%; $n = 5$). Recordings were done as described (*13*, *17*).
32. This observation and the lack of effect on the clustering of synaptic vesicles suggest that GST-amphSH3 does not perturb the function of proteins involved in the organization (*17*) or exocytosis of synaptic vesicles, in spite of the presence of proline-rich regions in many of these proteins [M. Linial, *Neuroreport* **5**, 2009 (1994)].
33. For GST-amphSH3–injected axons, the total EPSP amplitude decreased on average 77% (range 68 to 84%; $n = 5$) when the initial control period (5 min, 0.2 Hz stimulation) was compared with the end of a 30-min 5-Hz stimulation period. For GST-amphSH3mut–injected axons, the corresponding decrease was 46% (range 36 to 56%; $n = 4$), and for GST-injected axons it was 43% (range 38 to 49%; $n = 3$). The EPSPs studied had only a small electrotonic component in relation to the chemical component, and this relation was similar between the groups. A small chemical EPSP could be detected even at the end of the 30-min stimulation period after GST-amphSH3 injection. This indicates that GST-amphSH3 produces a kinetic inhibition of synaptic vesicle recycling, rather than a permanent blockade.
34. J. T. Buchanan, L. E. Moore, R. H. Hill, P. Wallén, S. Grillner, *Biol. Cybernet.* **67**, 123 (1992).
35. The "resting" dynamin pool, rather than being soluble in the cytoplasm, is accumulated at synaptic sites, presumably through interactions with components of the cytomatrix (*3*) [P. S. Estes *et al.*, *J. Neurosci.* **16**, 5443 (1996)]. This is consistent with our observation that GST-amphSH3, while inhibiting dynamin function, binds to and remains associated with the synaptic sites.
36. O. Shupliakov, P. Löw, H. Gad, L. Brodin, unpublished observation.
37. R. Fesce, F. Grohovaz, F. Valtorta, J. Meldolesi, *Trends Cell Biol.* **4**, 1 (1994); A. W. Henkel and W. J. Betz, *J. Neurosci.* **15**, 8246 (1995).
38. J. E. Heuser, *Cell Biol. Int. Rep.* **13**, 1063 (1989).
39. R. Scaife, I. Gout., M. D.Waterfield, R. L. Margolis, *EMBO J.* **13**, 2574 (1994); Z. Wang and M. F. Moran, *Science* **272**, 1935 (1996).
40. H. Shpetner, J. S. Herskovits, R. Vallee, *J. Biol. Chem.* **271**, 13 (1996).
41. V. Gundersen *et al.*, *J. Neurosci.* **15**, 4417 (1995).
42. Three-dimensional (3D) reconstructions were obtained from electronmicrographs of serial ultrathin sections (35 and 18 sections, respectively, for GST-amphSH3 and GST-amphSH3mut) with the use of MacStereology software. Only the main contours of the plasma membrane were included.

43. We thank A. Zhang and M. Butler for help and suggestions; P. Greengard, S. Grillner, and R. Petterson for advice and comments on the manuscript; S. J. Redman for providing computer software; and M. Bredmyr and H. Axegren for technical assistance. Supported by grants from the Swedish Medical Research Council (project 11287) and Jeanssons Stiftelser to L.B.; by grants from the Donaghue Foundation, the Human Frontier Science Program, and NIH (CA46128) to P.D.C.; and by postdoctoral fellowships from the Deutscher Akademischer Austauschdienst (to D.G.) and the United States Army Medical Research and Development Command (to C.D.).

25 November 1996; accepted 29 January 1997